Power Conditioner Efficiencies and Annual Performance Analyses with Partially Shaded Photovoltaic Generators Using Indoor Measurements and Shading Simulations

Cyril Allenspach,* Fabian Carigiet,* Arturo Bänziger, Andrin Schneider, and Franz Baumgartner*

Partially shaded photovoltaic systems operate with nonuniform conditions within the photovoltaic array, which lead to power losses. Module-level power electronics can potentially improve the performance of such photovoltaic systems. However, the potential performance increase compared to standard string inverter systems is site specific. To investigate this, power optimizer and string inverter efficiency measurements are conducted in the ZHAW indoor laboratory. With these results, simulations are performed for a module-level power electronics system with power optimizers at every module and a standard string inverter rooftop photovoltaic system. As a performance comparison, the P370 power optimizer and 3500H inverter are used for the module-level power electronics system and partial shading by a chimney is considered. For the standard string inverter system, the string inverter SUN2000-3.68KTL-L1, without the use of module-level power electronics, is chosen. The results of the annual simulations show a gain of the module-level power electronics system between –0.9% and 1.4% (14 modules) or –0.2% and 0.8% (13 modules), depending on the position of the chimney. Furthermore, the shading adaption efficiency, a method of quantifying the annual performance for shading situations by applying weightings to a few indoor measured performance values of power electronic components, is described.

1. Background on Module-Level Power Electronic

Module-level power electronics (MLPE) have gained such popularity over the last decade that their manufacturers now dominate the residential photovoltaic (PV) market in the USA and that they have significant market shares in many countries around the world.[1] As of now, nearly an amount of three digit in the millions of MLPE components is in operation worldwide,[2] whereas their market share has not shown signs of saturation. One of the unique abilities of MLPE is the operation of a PV module in the individual absolute maximum power point (MPP), unrelated on the setup of the respective PV string and especially so, in different shading conditions of each module.[3] Accordingly, it was one of the prime door opener in the market and assisted the widespread growth of the technology. However, in the literature there has not been shown clear evidence, which implicates that an annual performance increase of such PV rooftop systems equipped with MLPE in the double-digit range relative to standard string inverter (SINV) system is possible. In the few surveys that have been published,[4–6] one describes the topic of outdoor testing of typical row shading, which exists in large-scale PV installations.[7] Outdoor measurements of rooftop PV systems are important to show the operation performances under outdoor conditions, but there the measurement uncertainties and reproducibility are crucial factors, especially when the yield differences of the two compared systems are of the magnitude of a low one-digit number and thus close to the measurement uncertainties. Additionally, having an equal diffuse light condition on both installations, MLPE and SINV, but also the measurement of the related nominal power of the individual modules involved, is challenging. In contrast to the small number of publications on MLPE performance for shaded conditions, the topic of shading evaluation for PV systems, in general, has been dealt with in several studies. As a part of these analyses, a few, but comprehensive characterization methods for shaded PV systems were developed. One of these publications introduces and validates the measurable parameter for PV modules in shaded conditions, the so-called shading tolerability (ST), which is based on probability laws. In detail, it is a measure, which describes the capability of a PV module to withstand shading. Accordingly, it can be used to decide the adequate module technology for a PV installation to improve its corresponding

C. Allenspach, F. Carigiet, A. Bänziger, A. Schneider, F. Baumgartner
ZHAW School of Engineering
Institute of Energy Systems and Fluid-Engineering
Photovoltaic Systems Group
Zurich University of Applied Sciences
8401 Winterthur, Switzerland
E-mail: alls@zhaw.ch; cari@zhaw.ch; bauf@zhaw.ch

performance ratio (PR).[8] In a further publication, the formulation of the method was extended by its relation to thermal features and expanded for different temperature conditions. Additionally, the selection map for PV module installation based on ST was introduced, which offers a way to select the optimal PV module that is most probable to lead to a higher performance.[9] Another publication, which shows the complexity of shading, focuses on the yield of various PV modules with partial shading in an urban environment.[10] Furthermore, in a different publication, a simple model for the impacts of shading on the global irradiance on a rooftop was developed by the statistical analysis of around 48 000 rooftops in Uppsala, Sweden.[11] With the use of the previously mentioned shading tolerability, a comprehensive study of more than 3000 scenarios with the use of the Monte Carlo method and Latin hypercube sampling was conducted. In detail, the effects of partial shading for various module technologies (e.g., conventional, butterfly, shingle matrix) was analyzed, whereas the shading scenario was defined by a combination of a rectangular shade and several randomized shading clusters.[12] Consequently, it displays the difficulty of defining common shading scenarios, but shows that certain module technologies (e.g., shingle-type modules) perform on average significantly better in partially shaded conditions than others (e.g., conventional modules). Finally, on the topic of shading of PV systems, a publication focuses on the effects of shading due to soiling, whereby the significance of the environmental conditions in the location of a PV plant is underlined. Thus, surroundings with a high dust concentration (e.g., Canary Islands), or locations with snowfall such as the alpine region, can cause partial shading and impact the performance of the PV system.[13]

The Institute of Energy Systems and Fluid-Engineering (IEFE) at the Zurich University of Applied Sciences (ZHAW)[14] proposed in 2021 a new method of annual performance assessment of partially shaded PV systems by performing indoor component measurements and optical electrical shading simulation.[15] Thus, indoor performance tests on a SolarEdge P405 power optimizer under shaded and unshaded conditions were carried out at the ZHAW IEFE. The results of the 10-module PV plant showed that an MLPE system is expected to have a 2.8% lower yield than a comparable SINV system in unshaded and approximately 3.5% more energy when heavy shading by a dormer window is present.[16] For the mentioned laboratory tests, the voltage–current characteristics of the PV modules were calculated based on a clear-sky day in Switzerland and for both cases, PV module mismatches were neglected. Additional performance tests on a SolarEdge P370 power optimizer performed at the ZHAW IEFE revealed that a three-phase power optimizer system had 1.5% lower yield than a string inverter system in unshaded conditions, and 0.9% less when partially shaded by a chimney (indoor measurement uncertainty ±0.3%, $k = 1$).[17] Similar findings are provided by Bründlinger,[18] stating that the losses of unshaded systems with MLPE are typically 2–3% higher compared to the conventional string inverter topologies. These findings contrast heavily with manufacturers' datasheet statements claiming that these products ensure greater energy yields with "up to 25% more energy,"[19] or "increase in energy production of more than 36%."[20] A further conclusion of the ZHAW IEFE study, which received funding under SI/502247-01 by the Swiss Federal Office

of Energy (SFOE),[21] was that a quantifiable benefit of a MLPE system must be determined on a case-by-case basis. Although the results strongly depend on the individual efficiency of the power electronic components used, the general rule applies that in scenarios with extreme shading the MLPE system provides an advantage, whereas for light shading situations, lower yields than SINV systems are expected.[16] Still, the difficulty remains, as what degree of shading classifies as low or heavy shading. As a possibility, the method of the so-called shading tolerability could be used to simplify the process of such classifications in future analyses. However, so far, the case-by-case distinction would still be needed to be done, which significantly increases the complexity of PV system planning for four main reasons. First, PV system planners use annual yield simulation tools that typically simulate with hourly time steps and, due to time constraints, they are generally not able to run high-resolution simulations that analyze partial shading on the cell level of each PV module with appropriate loss models for MLPE.[15] Second, shading objects must be accurately measured in the field and transferred to 3D models, which would increase the PV system planning time. Third, the comparison of MLPE components is challenging, due to the absence of standards for reporting weighted average conversion efficiencies.[4] Power optimizer manufacturers report either peak or weighted conversion efficiencies but do not include details on the performance test conditions, such as operating points.[18,22] And finally, the total costs of MLPE systems are generally higher than string inverter solutions, due to the higher number of components and the additional time required for the installation of these components.[23,24] The case-by-case performance variation makes it difficult for planners to calculate when (or if) a potentially higher energy yield justifies higher system cost. These four challenges make, designing cost-effective PV systems for the final customer, a challenging task for PV system planners.

2. Indoor Laboratory Testing

In the IEFE laboratory at the ZHAW, a measurement and testing setup for MLPE was developed, which can be operated as a state-of-the-art residential PV plant consisting of 10 PV modules. The measurement system can mimic unshaded and shaded PV modules with the use of 10 solar array simulators (SAS) by providing different current–voltage (I–V) curve settings, according to the irradiance and temperature conditions on the PV module level.

2.1. System Setup

Every workstation has several types of MLPE by different manufacturers installed, which are powered by a Keysight E4261A-J01 SAS,[25] and measured with a Power Analyzer PPA1530 at the electrical input and output terminals.[26] During testing, the desired operating points of the PV modules are entered in the SAS devices, which calculate respective I–V curves for the given inputs to each MLPE. Accordingly, the SAS generate DC currents and voltages for the device-under-test based on PV I–V curves with a resolution of 4096 points. For a comprehensive overview, the electrical topology of the indoor laboratory setup is visualized

Figure 1. IEFE indoor laboratory MLPE setup and topology at the ZHAW SoE.

in **Figure 1**. Further description of the measurement setup is given in "Performance analysis of shaded PV module power electronic systems" and "Performance of new photovoltaic system designs."[15,27]

2.2. Power Optimizer Share of Losses

The losses in the power electronic converters occur in the individual components such as ohmic losses in the inductors and capacitors, ohmic and switching losses in the semiconductor switches, and the socket losses due to the power supplies of all active components, e.g., drives, control, and communication circuits. Equation (1)–(5) describe the power loss of the buck–boost-type power optimizer, which is used in the simulation as underlying model. In further detail, the model represents the steady-state losses of definite operating points with constant frequency. Accordingly, the effects of changes in frequency (i.e., frequency-related loss components) are not modeled explicitly; however, the losses by the switching operation are considered by the coefficients a and b.

$$D_{\text{cycle, buck}} = \frac{I_{\text{IN}}}{I_{\text{OUT}}} \tag{1}$$

$$D_{\text{cycle, boost}} = 1 - \frac{I_{\text{OUT}}}{I_{\text{IN}}} \tag{2}$$

$$P_{\text{loss, buck}}(k_I) = a + b \cdot U_{\text{IN}} \cdot I_{\text{IN}} \cdot D_{\text{cycle, buck}} + c \cdot I_{\text{OUT}}^2$$
$$+ d \cdot U_{\text{IN}}^2 \qquad \{k_I | k_I \geq 1.01\} \tag{3}$$

$$P_{\text{loss, boost}}(k_I) = a + b \cdot U_{\text{IN}} \cdot I_{\text{IN}} \cdot D_{\text{cycle, boost}} + c \cdot I_{\text{IN}}^2$$
$$+ d \cdot U_{\text{IN}}^2 \qquad \{k_I | k_I \leq 0.99\} \tag{4}$$

$$P_{\text{loss, passthrough}}(k_I) = a + c \cdot I_{\text{IN}}^2 \qquad \{k_I | 0.99 < k_I < 1.01\} \tag{5}$$

Generally, it is well known that a set of small power electronic components will lead to higher total losses compared to a single higher power device, e.g., DC/DC converter, as it is implemented in a SINV. Improvements of MLPE efficiency by the use of high bandgap semiconductors can reduce the gap.[28]

2.3. Measurement Results

With the use of high-precision power analyzers, the DC/DC efficiency of the MLPE is determined with an accuracy in the range of 0.2–0.5% ($k = 1$) in the ZHAW IEFE indoor laboratory. Accordingly, the whole operating range of buck–boost converter-type power optimizers was measured. In **Figure 2**, the DC/DC efficiencies of the type P370 for current ratios: $k_I = I_{\text{OUT}}/I_{\text{IN}}$ ranging from 0.6 to 1.65, and input power: P_{IN} ranging from 0 to 360 W, are visualized. In detail, the resulting efficiencies $\eta_{\text{DC/DC}}$ are between 95%, at low input power $P_{\text{IN}} \approx 18$ W, and 99.5%, at $P_{\text{IN}} = 98$ W and $k_I = 1$. However, distinct differences in efficiency can be identified between the region where $k_I = 1$ and all other operating points. In detail, in the narrow range around $k_I = 1$ (see red dots in Figure 2), the efficiencies are more than 0.8% higher than everywhere else,

due to the reason that the converter is not operating either in buck or boost mode, in the very few operation points. Therefore, the MOSFETs are inactive, and no switching losses occur. In other words, the input is directly connected to the output and only ohmic losses of the lines, inductor, and the MOSFET $R_{\text{DS (on)}}$ will occur.

The efficiency mapping in Figure 2 shows that values above 98% only occur in a limited field of the operating range, while the values mentioned by the manufacturers are either the maximum efficiency with 99.5% or the weighted efficiency of 98.9%.[22] Furthermore, the latter mentioned value could not be reached in the buck or boost mode, for which the component was designed. In detail, efficiency levels above 98.5% are limited to the range of $\frac{1}{3}$–$\frac{2}{3}$ of nominal power, and a $\frac{1}{4}$ more or less the number of optimizers used in the string, relative to $k = 1$. This results in 10–15 optimizer per string for the single-phase inverter, which is considerably less—for an efficient design—compared to the manufacturers possible range of 8–24.[22]

The measurement results of the P405 buck/boost power optimizer, illustrated in **Figure 3**, show a different picture at $k_U = 1$ compared to the P370 results in Figure 2. However notably, in Figure 3 the ratio of voltage and not current is given, and further, the visibility of the different operation modes is dependent on the measurement configuration and steady-state behavior. Nonetheless, the measured efficiency values at a static input voltage U_{IN} of 42 V show similar results to the P370 at 32 V, especially efficiency values below 97% at about one-tenth of full load.

Finally, it is important to realize that for determining the total MLPE system performance, the DC/AC efficiencies of the inverter would be needed to be multiplied with the values presented in this section, which would result in lower overall efficiencies.
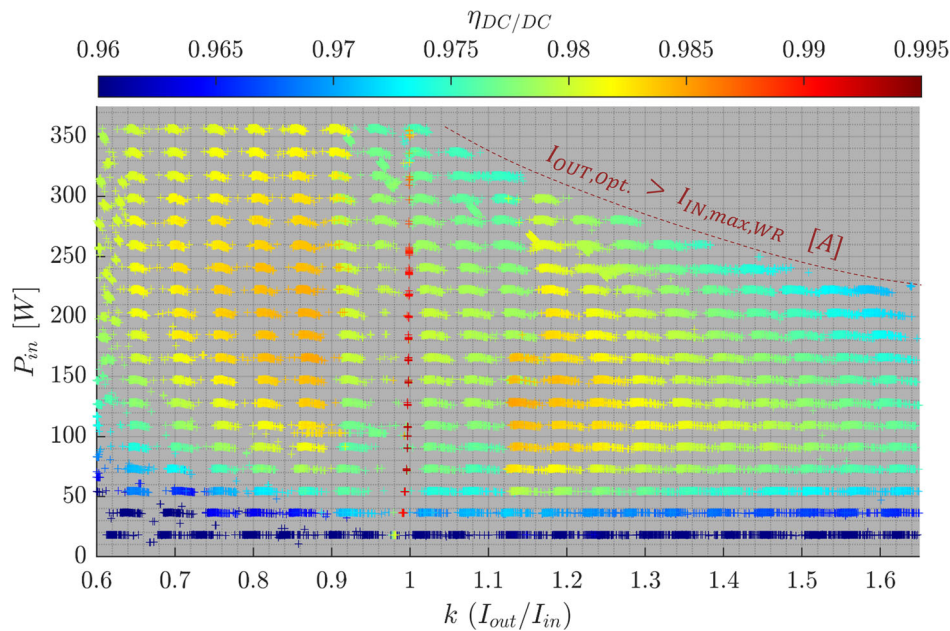
Figure 2. Static DC/DC efficiency measurement of the buck/boost-type power optimizer of model P370 at static input voltage $U_{\text{IN}} = 32$ V relative to the input/output current ratio.
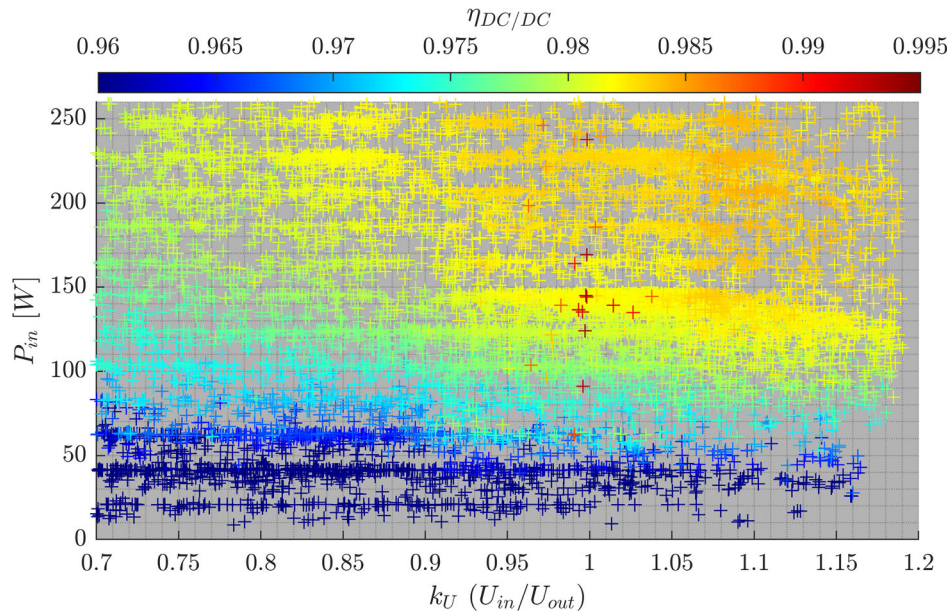
Figure 3. Static DC/DC efficiency measurement of the buck/boost-type power optimizer of model P405 at static input voltage $U_{IN} = 42$ V relative to the input/output current ratio.

3. High-Resolution Shading Simulation

A high-resolution shading analysis tool for the PV system simulations has been developed at ZHAW IEFE. In detail, the simulation tool was created in the Mathworks MATLAB environment,[29] whereby the simulated PV system, including shading objects, is modeled in 3D space, based on existing systems as shown in **Figure 4**,[30] and the shading situations are calculated for each position of the sun during the year with any temporal resolution. Global horizontal irradiance data provided by MeteoSwiss, the Swiss meteorological service,[31] are used and transposed to the PV plane for each time stamp using the transposition model by Ineichen and Perez.[32] The shadings on the PV module plane are calculated in such a

Figure 4. Single-family home with residential PV system (modules with 3 bypass diodes) and shading objects of type chimney and ventilation pipe. The 13 kWp PV plant was implemented by PV installer in Switzerland. Reproduced with permission.[30] Copyright 2022, Alsona AG.

way that there was no rasterization of the module plane, resulting in the highest possible resolution. Accordingly, the accuracy of the shading is only dependent on how accurate the convex shading object is modeled. Furthermore, based on the shading situation at each time step, the reduction of direct irradiance is determined for each solar cell in each PV module. Finally, the reduced direct irradiance together with the diffuse light, the ambient temperature, and the electrical configuration of the PV modules, with 60 standard 6 inch cells and 3 bypass diodes, in the string is used to calculate the I–V curves.

3.1. Simulation Concept

In the following figures, four distinct time steps of the PV shading simulation are visualized. In detail, the PV string and the chimney within it, based on Figure 4 (marked in red), were reproduced in the simulation environment, whereby it was modeled as self-contained PV system with a single-phase inverter. The simulated PV plant is south-facing with a 30° tilt and located, same as the actual system, in Switzerland (in the northern hemisphere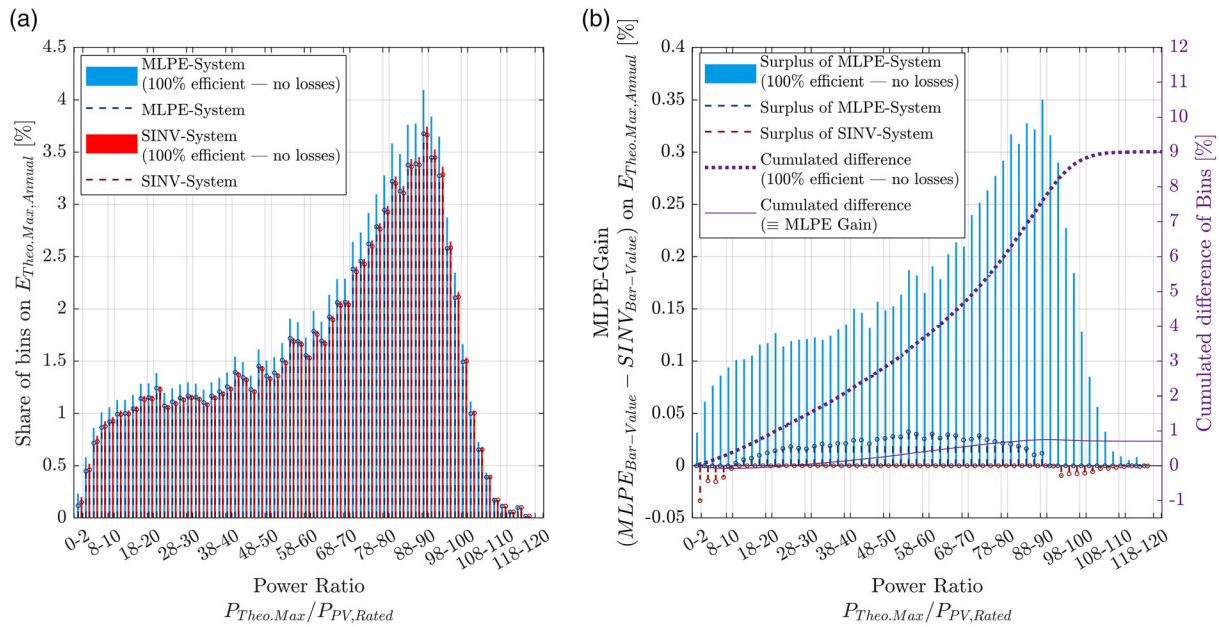), but with meteorological data from Kloten, Zurich. Furthermore, the PV plant was simulated simultaneously for two different system types, where one is a SINV-based system and the other MLPE based, for which power optimizers are used at every PV module. As underlying performance models, the simulation used the SUN2000-3.68KTL-L1 for the SINV[33] and the SE3500H with P370 power optimizer for the MLPE system.[22,34] Within the previously mentioned figures, the impacts of shading by the chimney are visualized for different time stamps from 09:40 to 12:15 during August 1, 2018. On the top left at each of the mentioned figures, the I–V curve of the PV module 11 (see Figure 4) is drawn. Therein, the circles show the MPP of the mentioned module. In **Figure 5**, the partial shading of the chimney reaches a maximum of 2.2% shading of a single most shaded cell in module 11. This instance represents the maximum amount of shading, where the SINV is still capable to track the same MPP at module 11 as the MLPE system. Accordingly, in

Figure 6. Second time step of the simulated PV system at 11:05 of August 1, 2018 (same shading scenario as described in the caption of Figure 5).

time step of the simulation, the MLPE system is able to track a greater MPP than the SINV. This is due to the restriction by the DC current of the module string, which is in series configuration. If the SINV would track the same MPP as the MLPE, powering the single shaded PV module, the current of all the unaffected modules would be reduced to a magnitude, where a disadvantageous smaller overall power output $P_{OUT, SINV–Sys}$ would occur. Consequently, the MLPE system will improve the output power, $P_{OUT, Mod}$, of module 11 in the duration from 09:41 to 11:05. However, the power output of the whole system $P_{OUT, MLPE–Sys}$ might not be increased depending on the losses in the individual moments caused by the additional conversion step of the MLPE at each module together with the subsequently needed DC/AC inverter.

In **Figure 6**, the shadow has moved further on the module 11, whereby the maximum magnitude of shading of the most shaded cell in the module substring has increased to 58.4%. As a result, the MPP at 35 V is now only a local maximum, whereby the new global maximum of the module now lies at approximately 19 V and at 9.3 A, which is the same current passing through all the unshaded PV modules. Consequently, the SINV now tracks the same MPP of module 11 as the MLPE system, whereas no additional yield gain is realized, but the additional conversion losses of each single power optimizer remain. The next moment, when the MLPE is capable of improving the yield gain of module 11, is 45 min later at 11:50, which is shown in **Figure 7**. In detail, the shading of the most shaded cell in a cell substring has decreased to a value of 56.8%, which leads to the global module MPP at 35 V. Once again, the MLPE is in favor in terms of efficiency. Another 25 min later, as visualized in **Figure 8**, the partial shading has decreased to 4.9%, at which point the SINV is once more able to track the same MPP without reducing the output power of all other unshaded modules significantly. In summary, the yield gain of the MLPE system is limited to a certain level of partial shading, which depends on the number of modules in the PV string, as well as on the prevailing irradiance, and which occurs only for a small period of the shading event.

Figure 5. First time step of the simulated PV system at 09:40 of August 1, 2018 (relating to sun position and weather data in Zürich). The shading and current–voltage characteristic of module 11 (outlined in red) is shown in detail on top of the 3D overview behind the chimney.

Figure 7. Third time step of the simulated PV system at 11:50 of August 1, 2018 (same shading scenario as described in the caption of Figure 5).

Figure 8. Fourth time step of the simulated PV system at 12:15 of August 1, 2018 (same shading scenario as described in the caption of Figure 5).

4. Shading Adaption Efficiency

Due to the reason that installers do not have the time or the required tools to analyze every PV system they design with a high-resolution shading simulation, a new measure is defined here, which enables the comparison of SINV and MLPE systems, each with their individual efficiencies. In the following section, an approach is presented to quantify the electrical output of the system relative to the highest possible DC input power. This is reached if every PV module is individually tracked at their absolute MPP without any conversion losses.

4.1. Proposed Concept

The described method was proposed as shading adaption efficiency (SAE), which is defined as the ratio of the output AC power to the maximum available DC power.[15] That DC power corresponds to the sum of all the individual PV modules k in the string, if all of them are operated in their individual absolute MPP. Therefore, this hypothetical DC power is identical to the output of a PV system, which is operated by 100% efficient DC/DC converters and inverters. In the laboratory setup described in Section 2, this ratio $\eta_{\mathrm{shad,a},n}$ will be calculated by the measured AC output power P_{AC} in a characteristic shading situation a, which is powered by specific I–V characteristics of such partially shaded and unshaded PV modules in the string. According to the denominator of Equation (6), the DC powers of each PV module tracked at their individual MPP will be measured in the lab and aggregated to the total DC input power of all k PV modules. When testing SINV systems, the measured DC input power at the plugs of the inverter will always be smaller or equal to the term, $\sum_{i=0}^{k} P_{\mathrm{mod},i}$. Smaller values can be expected in situations, where the DC string current prevents that every PV module is operated in their absolute MPP.

$$\eta_{\mathrm{shad,a},n} = \frac{P_{\mathrm{AC},n}}{\sum_{i=1}^{k} P_{\mathrm{mod},i,n}} \tag{6}$$

Equation (6) holds for an individual point in time n. The goal is to determine the annual average $\eta_{\mathrm{shad,a},n}$, which would require a large amount of indoor measurements. In order to reduce the number of measurements, only a few typical shading moments in a year should be measured and weighted accordingly. In other words, the efficiencies of the limited set of operating points n, at a characteristic shading situation a, are multiplied by their weighting factors and added up, as given in Equation (7).

$$\eta_{\mathrm{shad,a}} = \sum_{n=1}^{N} \eta_{\mathrm{shad,a},n} \cdot w_{\mathrm{shad,a},n} \tag{7}$$

The characteristic shading situations a will be identified by the binning of the annual system yields, and then found at several moments n in the annual mapping and marked by the numbers therein. Meanwhile, the weighting factors are representations of the energy amount during the year at similar SAEs, which are different for MLPE and SINV. A similar approach is found by the established calculations of the average string inverter efficiency according to the standards, based on the irradiance binning at different locations, such as the European efficiency η_{EURO} or California inverter efficiency η_{CEC}.[35,36]

4.2. Derivation of Weighting Factors for Annual Shading Performance

For the 13-module PV system setup, which was presented in Section 3.1, the annual simulation was performed. In detail, the performance model of the SUN2000-3.68KTL-L1 ($\eta_{\mathrm{EURO}} = 97.3\%$[33]) was chosen as SINV reference and the SE3500H ($\eta_{\mathrm{EURO}} = 98.8\%$[34]) with P370 power optimizer as MLPE system. In order to identify appropriate weighting factors $w_{\mathrm{shad,a},n}$ for the SAE in Equation (7), the yield, of every simulated time step of the annual simulation of the SINV and MLPE system, is allocated into bars as shown in **Figure 9**a. These bars are created based on the ratio of the theoretical maximum power of

Figure 9. a) Annual yield of the SINV and MLPE system, once for the 100% efficient and once for the effective yields after losses, is allocated in 2% bins. These bins represent relative values, based on the ratio of theoretical maximum power of each time stamp to the rated power of the PV plant. The yield is shown as the share of each bin on the total, theoretical maximum energy of the PV plant. b) The yield differences of the SINV and MLPE bins of (a) are visualized. Additionally, the cumulative sum of these differences are shown by lines and their values are based on the second *y*-axis on the right.

each time stamp (here in 5 min intervals), $P_{\text{MLPE-noLoss, Max}}$, to the rated power of the PV plant, $P_{\text{PV, rated}}$, whereas each bar represents 2% within the range of ratios (i.e., 0–2% to 118–120%). On the other hand, the height of each bar is defined by its yield share on the theoretical maximum annual yield without power electronic losses, $E_{\text{MLPE-noLoss, Max, Annual}}$. Within Figure 9a, the results of the theoretical, 100% efficient MLPE system indicate higher yields for every power ratio $P_{\text{MLPE-noLoss, Max}}/P_{\text{PV, rated}}$, which shows the hypothetical benefit of the module-level tracking. However, for the real MLPE yield, the difference has shrunk significantly, due to the higher losses of the MLPE components compared to the SINV system. Accordingly, the real yield of the SINV system is higher than the real MLPE for a power ratio above 92%. This is owing to the fact that the SINV performs better in situations when little to no shading occurs, which is the case for the 13-module PV plant during noon, when the prevailing irradiance conditions offer the highest yields. The mentioned differences can be seen in more detail in Figure 9b, where the surplus yield of the systems for every bin of Figure 9a is visualized. Within Figure 9b, the filled out bar in blue represents the difference of the theoretical 100% efficient PV systems without losses, which shows that theoretically the MLPE system has always a higher performance. However, the difference of the systems with losses visualised by the red and blue dashed bars, show a different result. In reality for the analysed case, the SINV will perform better for power ratios 0–10% and above 94%. Furthermore, based on the second *y*-axis (in purple), the cumulative difference of the 100% efficient systems is shown as a dotted line, whereas the effective, cumulative difference is displayed as a solid line. In detail, the cumulative difference

of the 100% efficient systems results in 9.1% and the effective difference in 0.8%, which shows the higher overall performance of the MLPE system, but underlines the additional losses caused by the greater number of power electronic devices. Now, for the definition of weighting factors $w_{\text{shad,a,n}}$ of the SAE, the number of bars must be reduced (e.g., to 6 bars), whereby their individual shares on $E_{\text{MLPE-noLoss, Max, Annual}}$ will represent the weighting values. Meanwhile, for every resulting bar, one strategically chosen operating point will be defined to represent a characteristic shading situation *a* with an efficiency $\eta_{\text{shad, a, n}}$ and thereby exemplify the performance of the respective bars. As a consequence, the characteristic shading situations *a*, their weighting factors $w_{\text{shad,a,n}}$, and correlating operating points will be identified. Notably, the results are only valid for the previously described location of the PV plant and its corresponding conditions.

In **Table 1**, the results of the previously described reduction of bars and the definition of corresponding, characteristic shading moments *n*, are presented. In detail, the bars were reduced to six ranges (shown in row 2), which shares on $E_{\text{MLPE-noLoss, Max, Annual}}$ resulted in the weightings $w_{\text{shad,a,n}}$ of row 3 in Table 1. Within each of the six bars, a representative shading moment *n* was chosen, for which the respective $\eta_{\text{shad, a, n}}$ of the system-under-test shall be identified.

For the previously described 13-module PV system, which results are shown in Figure 9, the SAE calculation was performed. In further detail, the Equation (6) was applied for the shading moments *n* described in Table 1 and thus, by using Equation (7) with the defined $w_{\text{shad,a,n}}$, the SAE was identified. The resulting MLPE gain and, in addition, the simulated results

Table 1. Description of the defined weighting factors $w_{shad,a,n}$ and characteristic shading moments n.

Shading moments n	1	2	3	4	5	6
Power ratio [%]						
$P_{MLPE-noLoss,Max}/P_{PV,rated}$	0–30	31–44	45–60	61–78	79–88	89–120
Weighting factors						
$w_{shad,a,n}$	0.16	0.10	0.13	0.22	0.18	0.21
Date + Time of shading moments n	July 3, 10:55	April 3, 08:55	August 13, 10:00	September 4, 14:50	June 9, 14:35	April 17, 12:20

which represent the target values are presented in **Table 2**. Although the totals of the SAE calculation differ from its target values by 0.45 and 0.48%, the difference of the MLPE gain results in only 0.04%.

For the validation of the weightings $w_{shad,a,n}$ and shading moments n, the same PV plant was simulated with components that show a lower overall efficiency. In detail, the performance model of the SB3.6-1AV-41 inverter was used for the SINV system, and for the MLPE system, the SE3500 (non-HD-wave) inverter was utilized, while the power optimizer model remained the same. Once again, the resulting SAEs in **Table 3** show values, which are 0.44 or 0.47% higher than the target values, i.e., the simulated annual SAE. However, the resulting MLPE gain nearly matches the target value with a difference of −0.02%. Consequently, the characteristic shading moments n are good indicators for the comparison of MLPE and SINV system components at different efficiency values. However, a future analysis of different characteristic shading moments might result in SAEs, which coincide more accurately with the target values. Nonetheless, for the purpose of demonstrating the SAE method

with the mentioned example, the chosen values can be seen as sufficiently precise for now. Additionally, the MPPs of each PV module and every characteristic shading moment, n, are presented in **Table 4** for the sake of completeness.

4.3. Resulting System Efficiencies

The corresponding efficiency results for both the SINV and MLPE system are visualized as annual mappings in **Figure 10**. The coloring shows the SAEs of the mentioned systems for every day of a year and every moment of a day to identify the most beneficial performance of either SINV or MLPE. For the definition of the SAE, the value of the individual weighting factors, $w_{shad,a,1}$, $w_{shad,a,2}$ to $w_{shad,a,n}$, are found by aggregating similar operating points over the whole year, as described in Section 4.2. For the shading situation a, the typical operating points are marked in Figure 10. With the annual mapping of the SAE values, it is further possible to analyze the effects of shading on the performance of a system or to compare the two systems in detail and at any moment during the year. It can

Table 2. Defined weighting factors, operating points, and corresponding simulated shading efficiency values. SINV: SUN2000-3.68KTL-L1—MLPE: SE3500H (HD-wave) + P370. Additionally, the total system efficiencies $\eta_{x,Total}$ of the SINV and MLPE are shown, while the corresponding, tracked input power P_{MPP} was different for each system.

Operating points	1	2	3	4	5	6	Resulting SAE [%]	Resulting MLPE gain [%]	Annual SAE [%] (5 min sim.)	Annual [%] MLPE gain (5 min sim.)
Weighting factors	0.16	0.10	0.13	0.22	0.18	0.21				
MLPE SAE [%]	96.60	97.13	97.77	97.49	96.96	96.65	**97.08**		96.63	
								0.76		0.80
SINV SAE [%]	97.65	94.57	89.09	97.95	97.85	97.69	**96.34**		95.86	
MLPE efficiency $\eta_{MLPE,Total}$ [%]	96.60	97.13	97.77	97.49	96.96	96.65				
SINV efficiency $\eta_{SINV,Total}$ [%]	97.65	98.17	98.18	97.95	97.85	97.69				

Table 3. Validation set for the defined weighting factors, operating points, and corresponding simulated shading efficiency values. SINV: SB3.6-1AV-41—MLPE: SE3500 + P370.

Operating points	1	2	3	4	5	6	Resulting SAE [%]	Resulting MLPE gain [%]	Annual SAE [%] (5 min sim.)	Annual [%] MLPE gain (5 min sim.)
Weighting factors	0.16	0.10	0.13	0.22	0.18	0.21				
MLPE SAE [%]	94.96	95.51	95.33	94.74	94.41	94.59	**94.84**		94.40	
								−1.79		−1.77
SINV SAE [%]	96.18	95.34	95.87	97.08	97.03	96.94	**96.57**		96.10	

Table 4. MPP values of each PV module for the characteristic shading moments n of the chimney case applied in 1–3.

	I_{MPP} [A]	V_{MPP} [V]	I_{MPP} [A]	V_{MPP} [V]	I_{MPP} [A]	V_{MPP} [V]
	1		2		3	
Modules 1–6, 8–10, and 12–13	2.06	35.37	4.19	35.37	5.70	35.37
Module 7	2.06	35.30	1.55	38.81	4.59	34.61
Module 11	2.06	35.37	4.18	23.40	5.07	34.74
	4		5		6	
Modules 1–13 (all PV modules)	7.90	31.71	9.26	30.44	10.81	30.26

be stated that the MLPE system (left-hand side in Figure 10a) is less impacted by the shading than the SINV (Figure 10b). However, the SINV performance is higher between 12:00 and 15:30 because there is no shading on the PV modules (as described in Section 4.2). During these times also high energy yields occur. The annual average SAE of the MLPE results in 96.6% and for the SINV 95.9%. Consequently, the MLPE can improve the performance by 0.7% in this particular situation, where the chimney is directly positioned next to the PV system.

In **Figure 11**, the mapping of the efficiency difference between the MLPE and SINV system relative to the annual DC yield of MLPE is visualized. Notably, the difference was weighted based on the relative share of each time stamp on the theoretical maximum yield $E_{MLPE-noLoss, Max, Annual}$. Accordingly, the differences $\Delta Gain_{MLPE, E-wgt.}$ with a stronger impact on the annual energy yield are colored more intensively.
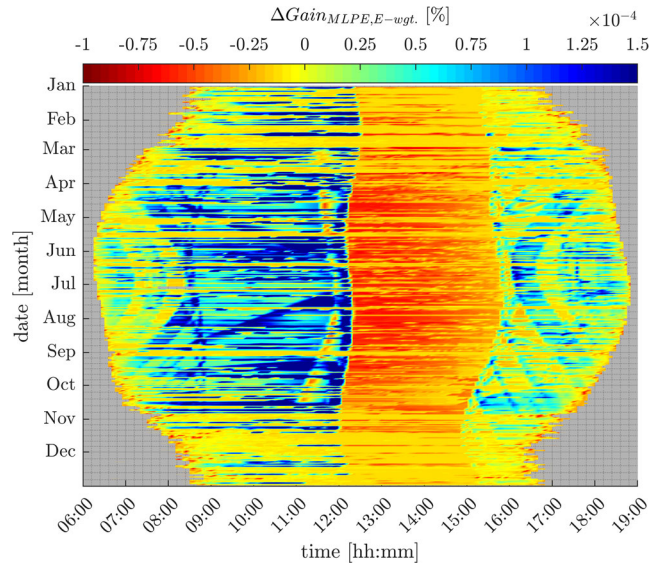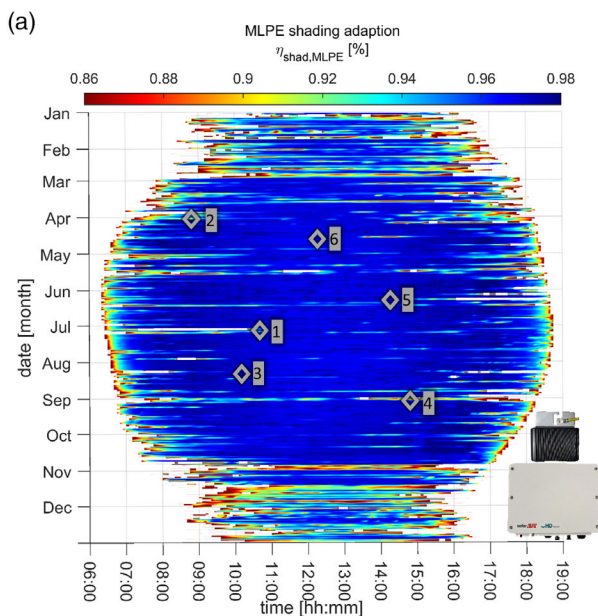
Figure 11. Energy-weighted MLPE gain mapping for days in the year and every time step of the day. The resulting MLPE gain values are weighted based on their impact on the PV energy yield of the plant for the whole year. Corresponding MLPE gains are based on the color bar on top and colored correspondingly.

5. Sensitivity Analysis

The position of the shading object relative to the PV plant has a substantial impact on the annual energy yield of the plant, but also the potential gain of the MLPE system. Generally, the closer the object is placed to the PV modules and the more modules are partially shaded around the zenith of the days, and especially
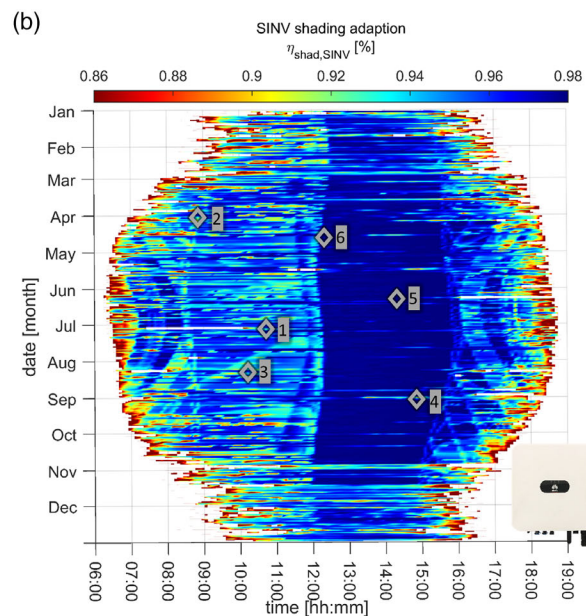
Figure 10. Momentary SAEs for the MLPE a) and SINV system b) as a mapping of days in the year and every time step of the day. The efficiency values are based on the color bar on top and colored correspondingly. The device images, whose performance models are used in the simulation, are shown next to the mappings.

during summertime, the higher the yield gains of the MLPE system compared to the SINV system. However, by placing the modules further away from the shading object, the yield of the SINV is increased and, therefore, the MLPE yield gain decreases. The SINV might even perform better than the MLPE system in the annual yield analysis, if no relevant shading occurs at high daily irradiance situations. In the analysis, only the position of the shading object, a chimney with a side length of 50 cm, in relation to the PV modules was varied 4 times 30 cm horizontally and each time also 35 cm vertically along the PV plane. Accordingly, the influence by changes in number of bypass diodes, module or cell technology or orientation is not analyzed. In the following figures, the annual MLPE yield gain is visualized with boxes, whereby their location represents the position of the chimney and where their colors correspond to the magnitude of gain in percent. In **Figure 12**, the same PV system setup as in the previous section is visualized. However, an additional PV module was placed behind the chimney and the chimney position was varied. As a result, with a position of the chimney in the lower left corner, the MLPE system performed 1.4% better than the SINV system. At this chimney position, the PV plant observes the highest amount of shading, whereby the benefits of the MLPE tracking come into effect for a major portion of the year. The mentioned annual result with the maximum MLPE yield gain and the result of the position with the lowest MLPE yield gain are further described in **Table 5**. Therein, also the energy yield of the cases is mentioned relative to the yield of the PV plant, when no shading occurs.

Another simulation with the same setup was performed, but this time the underlying SINV model was replaced by the SB3.6-1AV-41 (η_{EURO} = 96.5%) inverter from SMA.[37] For the MLPE system, the inverter was changed to the SE3500 (non-HD-wave) (η_{EURO} = 97.5%),[38] whereas the power optimizers remained the same. Both inverters show lower general performances than the components that were used in the simulation

Table 5. Annual simulation results of the 14-module PV plant (heavy shading) for the configuration I: SUN2000-3.68KTL-L1 (SINV)— SE3500H + P370 (MLPE). For the chimney positions resulting in the maximum and minimum MLPE yield gain, the results are presented. Within the column "Relative yield to I.ref1 [%]," the result of the unshaded SINV system was chosen as reference value for the other cases and therefore it shows a bold 100.

Cases	Components	SAE [%]	Relative yield to I.ref1 [%]	MLPE gain [%]
I.a: SINV maxGain	3.68KTL-L1	95.2	93.0	1.4
I.b: MLPE maxGain	SE3500H + P370	96.5	94.3	
I.c: SINV minGain	3.68KTL-L1	95.7	94.1	0.9
I.d: MLPE minGain	SE3500H + P370	96.5	94.8	
I.ref1: SINV unshaded	3.68KTL-L1	97.4	**100**	−1.0
I.ref2: MLPE unshaded	SE3500H + P370	96.4	99.0	

of Figure 12. Most notably in this case, as shown in **Figure 13**, the MLPE system cannot achieve yield gains compared to the SINV, although there are heavy shading conditions on the PV plant. The maximum yield gain results in a minuscule value above zero. On the other hand, the minimum yield gain results in −0.6%, which is realized at the chimney position with the minimal shading effect. Once again, the mentioned results are illustrated in **Table 6**, where also the relative yield of the cases to the PV plant without shading is shown.

With focus on the real PV system, presented in Section 3, the same simulations are carried out, but only with the 13 modules that are actually installed on this particular roof. Once again, the underlying system setup with SINV: SUN2000-3.68KTL-L1 (η_{EURO} = 97.3%) and MLPE: SE3500H (η_{EURO} = 98.8%) with P370 was chosen. According to **Figure 14**, the maximum MLPE yield gain resulted in 0.79%, whereby the respective chimney position correlates with the chimney position on the actual rooftop installation. Notably, this chimney position causes the
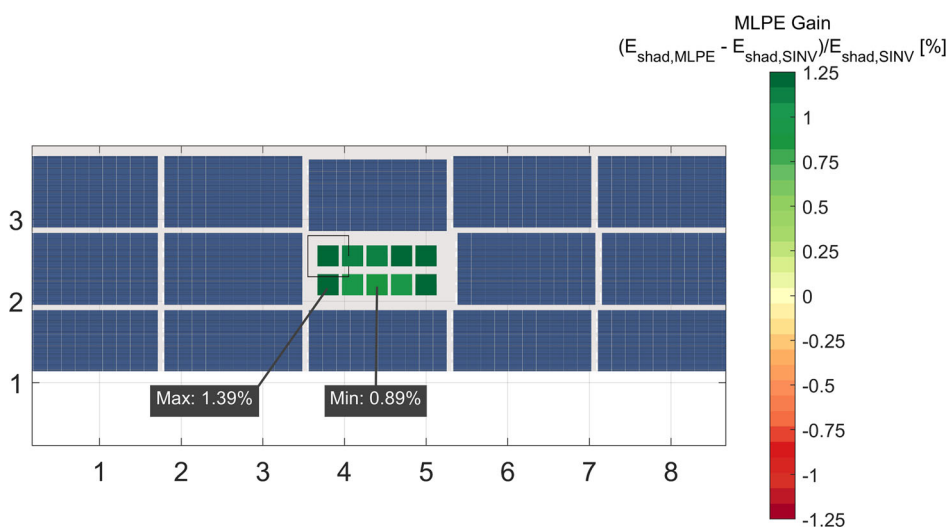

Figure 12. Comparison of the SINV: SUN2000-3.68KTL-L1 and MLPE: SE3500H with P370 power optimizer for a 14-module residential PV plant. Annual MLPE yield gain for 10 chimney positions visualized as boxes and their magnitude indicated by color bar. Minimum 0.9% and maximum MLPE yield gain 1.4% are denoted by gray text boxes.
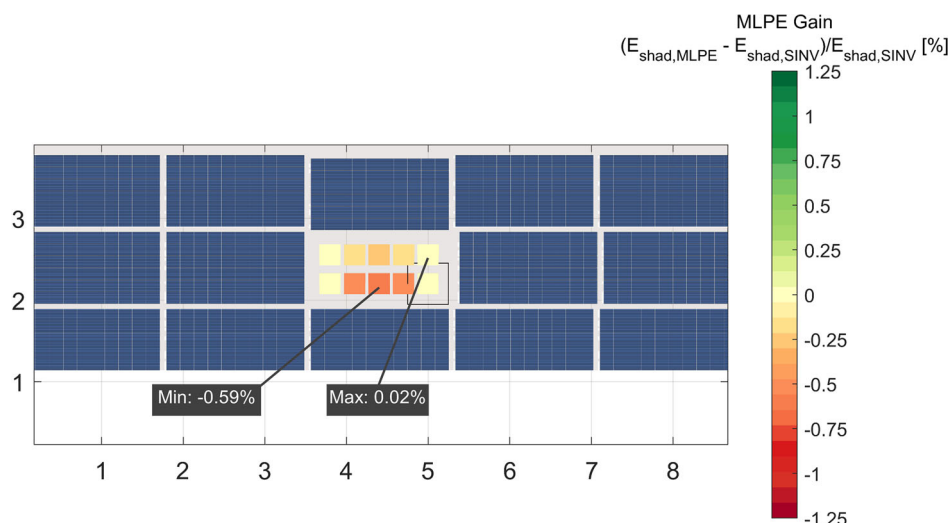
Figure 13. Comparison of the SINV: SB3.6-1AV-41 and MLPE: SE3500 (non-HD-wave) with P370 power optimizer for a 14-module residential PV plant. Annual MLPE yield gain for 10 chimney positions visualized as boxes and their magnitude indicated by color bar. Minimum −0.6% and maximum MLPE yield gain 0.02% are denoted by gray text boxes.

Table 6. Annual simulation results of the 14-module PV plant (heavy shading) for the configuration II: SB3.6-1AV-41 (SINV)—SE3500 (non-HD-wave) + P370 (MLPE). For the chimney positions resulting in the maximum and minimum MLPE yield gain, the results are presented. Within the column "Relative yield to II.ref1 [%]," the result of the unshaded SINV system was chosen as reference value for the other cases and therefore it shows a bold 100.

Cases	Components	SAE [%]	Relative yield to II.ref1 [%]	MLPE gain [%]
II.a: SINV maxGain	SB3.5	94.2	92.4	0
II.b: MLPE maxGain	SE3500 + P370	94.2	92.4	
II.c: SINV minGain	SB3.5	94.7	94.0	−0.6
II.d: MLPE minGain	SE3500 + P370	94.1	93.4	
II.ref1: SINV unshaded	SB3.5	96.5	**100**	−2.5
II.ref2: MLPE unshaded	SE3500 + P370	94.1	97.5	

greatest amount of shading, which is why the MLPE shows improved performance. On the other hand, if the distance between the PV modules on the left side of the roof and the chimney was greater, the MLPE gain could have been −0.2%, meaning that the SINV system would perform better. With this in mind, that position would also cause a greater annual yield compared to the case with the maximum MLPE yield. This holds true not only for the SINV, but also for the MLPE system, as can be identified by the values of column 4 of **Table 7**, which shows the relative yields to the unshaded case.

In order to be able to decide whether the MLPE or the SINV system is performing better on an annual basis, the individual real efficiency is relevant, as it is proven by the results of Table 7. Additionally, in **Table 8**, the annual results of the 13-module PV plant with inverters with a lower general performance—SB3.6-1AV-41 (SINV) | SE3500 (non-HD-wave) + P370 (MLPE) —are shown for the sake of completeness.

6. Discussion and Outlook

Partial shading of PV systems has a significant impact on the annual performance. Additionally, the analyses of different plant configurations are time-consuming. Up to now, there is no method available for installers to identify, which system components are best suited for certain specific situations they encounter. With the presented new approach, the SAE can be used to assess the few most common shading cases, which would need to be defined in future works as well as in standards. These cases will then stand as a benchmark for the comparison of power electronic components of string inverter (SINV) and MLPE systems (MLPE), which will help the decision-making of installers, especially for the planning of residential rooftop PV plants. On the other hand, the method offers an approach for manufacturers to evaluate their system components in the benchmark situations by simply testing and measuring their components efficiency at a small number of standardized operating points, representing a few defined moments in a year, in order to assess the annual yield of the characteristic shading cases.

6.1. Findings

For a PV string consisting of 13 PV modules, an annual shading simulation for the SINV and MLPE system was conducted. In detail, this PV string exists in reality and is installed on a single family house in Switzerland, whereby a chimney in the middle of the PV plant causes partial shading. For one simulated day in August, four distinct moments of shading are presented and discussed in detail. The sequence of partial shading situations within the duration of 2 h and 35 min visualizes that the MLPE components do not always offer an improved yield when shading occurs. In detail, the MLPE system, for which power optimizers are installed at every PV module, enables an
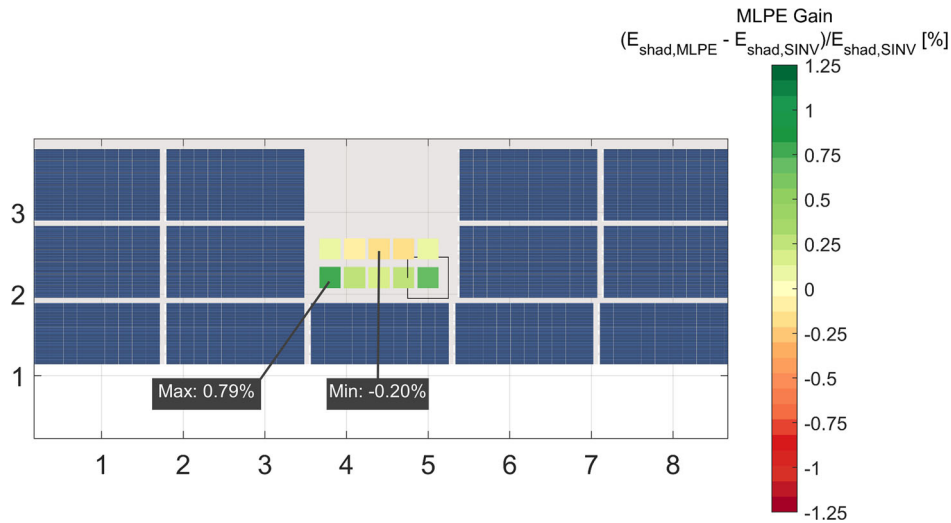
Figure 14. Comparison of the SINV: SUN2000-3.68KTL-L1 and MLPE: SE3500H with P370 power optimizer for the actual, 13-module residential PV setup (in Figure 4). Annual MLPE yield gain for 10 chimney positions visualized as boxes and their magnitude indicated by color bar. Minimum –0.2% and maximum MLPE yield gain 0.8% are denoted by gray text boxes.

Table 7. Annual simulation results of the 13-module PV plant (light shading) for the configuration I: SUN2000-3.68KTL-L1 (SINV)—SE3500H + P370 (MLPE). For the chimney positions resulting in the maximum and minimum MLPE yield gain, the results are presented. Within the column "Relative yield to III.ref1 [%]," the result of the unshaded SINV system was chosen as reference value for the other cases and therefore it shows a bold 100.

Cases	Components	SAE [%]	Relative yield to III.ref1 [%]	MLPE gain [%]
III.a: SINV maxGain	3.68KTL-L1	95.9	94.9	0.8
III.b: MLPE maxGain	SE3500H + P370	96.6	95.6	
III.c: SINV minGain	3.68KTL-L1	96.9	97.4	−0.2
III.d: MLPE minGain	SE3500H + P370	96.7	97.2	
III.ref1: SINV unshaded	3.68KTL-L1	97.6	**100**	−1.0
III.ref2: MLPE unshaded	SE3500H + P370	96.6	99.0	

Table 8. Annual simulation results of the 13-module PV plant (light shading) for the configuration II: SB3.6-1AV-41 (SINV)—SE3500 (non-HD-wave) + P370 (MLPE). For the chimney positions resulting in the maximum and minimum MLPE yield gain, the results are presented. Within the column "Relative yield to IV.ref1 [%]," the result of the unshaded SINV system was chosen as reference value for the other cases and therefore it shows a bold 100.

Cases	Components	SAE [%]	Relative yield to IV.ref1 [%]	MLPE gain [%]
IV.a: SINV maxGain	SB3.5	94.8	94.9	−0.4
IV.b: MLPE maxGain	SE3500 + P370	94.4	94.5	
IV.c: SINV minGain	SB3.5	95.8	97.4	−1.4
IV.d: MLPE minGain	SE3500 + P370	94.4	96.0	
IV.ref1: SINV unShade	SB3.5	96.5	**100**	−2.2
IV.ref2: MLPE unShade	SE3500 + P370	94.4	97.8	

increased yield of one PV module in a range of shading ratios between 2% and 56%. However, the amount varies with the magnitude of prevailing irradiance and the number of modules in the series connection with that module.

Furthermore, the methodology of the SAE is presented and realized for the previously mentioned PV system. Within the analysis, weighting factors are defined which are dependent on the location of the PV system (i.e., Switzerland), its corresponding conditions (e.g., climate), and the specific shading scenario. Accordingly, the method of the SAE was introduced and the corresponding calculation verified by the mentioned case. Thus, further analyses can be conducted in future to identify weighting factors for other climate zones and shading cases. Consequently, a small set of such cases will be defined within a technical specification or standard, which will enable manufacturers to test their products in a laboratory environment and to state the resulting shading adaption values within their datasheets similar to the CEC or EURO efficiency for inverters. Finally, installers will have the necessary quantities to compare products and technologies performance-wise to guarantee a PV installation most suited to their customers' needs.

For the shading scenario of the PV installation in Switzerland, the annual performance is visualized as a mapping of momentary SAE values. In summary, the performance of the MLPE system is less impacted by the shading; however, the SINV system has a higher yield during 12:00 to 15:30, as there is less shading present. Given these points, the resulting annual average SAE arrives at 96.6% for the MLPE and 95.9% for the SINV, which shows that the MLPE system performs approximately 0.7% better with the analyzed system configuration.

Moreover, the location of the chimney is varied, 4 times 30 cm horizontally and each time also 35 cm vertically along the PV plane, to be able to analyze the sensitivity of the annual results and in respect to the SAE. Most notably in the case of the 13-module PV system in Switzerland and the chimney position causing the highest degree of shading on the module plane, the

MLPE system shows an annual yield gain 0.8% compared to the SINV. However, if the chimney position is adjusted by 60 cm horizontally and 35 cm vertically, the lowest possible shading of the module plane occurs. Correspondingly, an improved tracking of the MLPE system is realized in fewer cases during the year, for which reason the SINV shows an annual yield 0.2% higher than the MLPE system. Consequently, the further the shading object is located from the PV plant and the less shade occurs during noon, the greater the performance of the SINV compared to MLPE system.

Generally, newer generations of components should be utilized, as they can offer at least 1% higher yields, regardless if MLPE or SINV configuration is used. Nonetheless, the performance of the HD-wave inverter (SE3500H) of the MLPE system with only the DC/AC stage, which has been measured and analyzed in detail at ZHAW, performs with a European efficiency η_{EURO} of 98.8%, significantly better than the predecessor model (SE3500) with $\eta_{EURO} = 97.5\%$. Unfortunately so far, the technology of the HD-wave model has not been implemented in current three-phase models, and is therefore limited to 10 kVA, or less, depending on the local regulations of asymmetric loading of power lines. Similarly, the SINV with a combined DC/DC and DC/AC stage, SUN2000-3.68-KTL-L1, offers a η_{EURO} of 97.3%, resulting in a fair comparison of the MLPE and SINV system. Furthermore, in the 13-module system, which showed less shading, especially during noon, the SINV (SUN2000-3.68-KTL-L1) had a higher performance than the MLPE system at three chimney positions. The distances to the PV modules were the greatest in these positions, whereas the chimney still caused shading on the PV modules. Accordingly in the mentioned cases, the additional losses of the power optimizers during the year were greater than the yield gain by their module-level tracking in times of shading, relative to the SINV. The mentioned losses might be reduced for an MLPE system, in which power optimizers are only installed at certain, most shaded modules, which is a system configuration that will be analyzed in future works.

6.2. Future Works

For further evaluation of specific shading situations, which are different to the future benchmark cases, an in-depth guideline is being developed to further support the PV system planners. Furthermore, the International Energy Agency (IEA) Task 13 ST2.5[39] is currently involved in the definition of the characteristic, benchmark shading situations, which will guarantee an objective standardization. Furthermore, within the IEC TC 82/WG 6,[40] the method of the SAE was presented. The method will support the development of future technical specifications and standards in accordance with the various international committees, consisting of the major manufacturers and researchers of the photovoltaic industry.

Acknowledgements

Conflict of Interest

The authors declare no conflict of interest.

Data Availability Statement

The data that support the findings of this study are available from the corresponding author upon reasonable request.

Keywords

[1] A. Gattlin, Investor's Business Daily **2022** (accessed: June 2022).
[2] SolarEdge Technologies Inc., www.solaredge.com/sites/default/files/se-fact-sheet-na.pdf (accessed: May 2022).
[3] C. Deline, B. Marion, J. Granata, S. Gonzalez, Technical report, National Renewable Energy Laboratory (NREL) and Sandia National Laboratories **2011**.
[4] C. Deline, S. MacAlpine, in *Proc. of the 2013 IEEE Energy Conversion Congress and Exposition* 2013, IEEE, New York, NY pp. 4801–4807.
[5] A. J. Hanson, C. Deline, S. M. MacAlpine, J. T. Stauth, C. R. Sullivan, *IEEE J. Photovoltaics* **2014**, *4*, 1618.
[6] K. Sinapis, C. Tzikas, G. Litjens, M. van den Donker, W. Folkerts, W. van Sark, A. Smets, *Sol. Energy* **2016**, *135*, 731.
[7] C. Deline, J. Meydbray, M. Donovan, Technical report, National Renewable Energy Laboratory (NREL) and PVEvolution Labs/DNV GL **2016**.
[8] H. Ziar, B. Asaei, S. Farhangi, M. Korevaar, O. Isabella, M. Zeman, *IEEE J. Photovoltaics* **2017**, *7*, 1390.
[9] S. Mishra, H. Ziar, O. Isabella, M. Zeman, *IEEE J. Photovoltaics* **2019**, *9*, 872.
[10] A. Calcabrini, R. Weegink, P. Manganiello, M. Zeman, O. Isabella, *Sol. Energy* **2021**, *225*, 726.
[11] S. Killinger, D. Lingfors, Y.-M. Saint-Drenan, P. Moraitis, W. van Sark, J. Taylor, N. A. Engerer, J. M. Bright, *Sol. Energy* **2018**, *173*, 1087.
[12] N. Klasen, F. Lux, J. Weber, T. Roessler, A. Kraft, *IEEE J. Photovoltaics* **2022**, *12*, 546.
[13] C. Schill, S. Brachmann, M. Koehl, *Sol. Energy* **2015**, *112*, 259.
[14] ZHAW School of Engineering (ZHAW), www.zhaw.ch/en/engineering/institutes-centres/iefe/renewable-energies/photovoltaics/ (accessed: May 2022).
[15] F. Baumgartner, R. Vogt, C. Allenspach, F. Carigiet, in *Proc. of the 38th European Photovoltaic Solar Energy Conf. and Exhibition (EUPVSEC), Online*, WIP Renewable Energies, Munich, Germany **2021**, pp. 650–654.
[16] C. Allenspach, V. G. de Echavarri Castro, S. Richter, C. Meier, F. Carigiet, F. Baumgartner, in *Proc. of the 37th European Photovoltaic Solar Energy Conf. and Exhibition (EUPVSEC)*, WIP Renewable Energies, Munich, Germany **2020**, pp. 1188–1194.

[17] C. Allenspach, A. Bänziger, A. Schneider, F. Carigiet, F. Baumgartner, in *20th Swiss National Photovoltaic Conf.*, Swisssolar, Zurich, Switzerland **2022**.

[18] R. Bründlinger, N. Henze, G. Lauss, J. Liu, in *Proc. of the 26th European Photovoltaic Solar Energy Conf. and Exhibition (EUPVSEC)*, WIP Renewable Energies, Munich, Germany **2011**, pp. 3204–3211.

[19] SolarEdge Technologies Inc., www.solaredge.com/sites/default/files/residential_catalogue_eng.pdf (accessed: June 2022).

[20] Tigo Energy Inc., www.tigoenergy.com//product/ts4-a-o (accessed June 2022).

[21] Swiss Federal Office of Energy (SFOE), EFFPVSHADE - Effizienzanalyse von dezentraler Photovoltaik Leistungselektronik bei Teilbeschattung [EFFPVSHADE - Analysis of efficiency of decentralized phototvoltaic power electronics under partial shading], SI/502247-01, 2021-2023.

[22] SolarEdge Technologies Inc., www.solaredge.com/sites/default/files/se-p-series-add-on-power-optimizer-datasheet.pdf (accessed: May 2022).

[23] I. Mehedi, Z. Salam, M. Ramli, V. Chin, H. Bassi, M. Rawa, M. Abdullah, *Renewable Sustainable Energy Rev.* **2021**, *146*, 111138.

[24] N. Dekker, M. Jansen, A. Burgers, M. Dörenkämper, R. Jonkman, R. van der Ven, E. Gramsbergen, in *Proc. of the 37th European Photovoltaic Solar Energy Conf. and Exhibition (EUPVSEC)*, WIP Renewable Energies, Munich, Germany **2020**, pp. 945–951.

[25] Keysight Technologies, www.keysight.com/ch/de/products/dc-power-supplies/dc-power-solutions/e4360-series-modular-solar-array-simulators.html (accessed: June 2022).

[26] Newtons4th Ltd., www.newtons4th.com/products/power-analyzers/ppa1500-precision-power-analyzer/ (accessed: May 2022).

[27] M. Littwin, U. Jahn, F. Baumgartner, M. Green, W. van Sark, C. Allenspach, E. Bamberger, C. Biba, C. Deline, D. Gfeller, S. M. Goldroodbari, M. Köntges, C. Messner, U. Muntwyler, R. Neukomm, D. Riley, D. Rivola, J. S. Stein, M. Trommsdorff, Technical Report Report IEA-PVPS T13-15:2021 (ISBN 978-3-907281-04-8), International Energy Agency (IEA) PVPS Task 13, **2021**.

[28] N.-C. Sintamarean, E.-P. Eni, F. Blaabjerg, R. Teodorescu, H. Wang, in *Proc. of the Inter. Power Electronics Conf. (IPEC ECCE Asia)*, IEEE, New York, NY **2014**, pp. 1912–1919.

[29] The Mathworks Inc., www.mathworks.com/products/MATLAB (accessed: June 2022).

[30] A. G. Alsona, www.alsona.ch (accessed: June 2022).

[31] Swiss Federal Office of Meteorology and Climatology (MeteoSwiss), www.meteoswiss.admin.ch/ (accessed: June 2022).

[32] P. Ineichen, R. R. Perez, E. Maxwell, R. D. Seals, A. Zelenka, *ASHRAE Trans. Res.* **1992**, *98*, 354.

[33] Huawei Technologies Co., Ltd, solar.huawei.com/en-GB/download?p= (accessed: June 2022).

[34] Solaredge Technologies Ltd., www.solaredge.com/sites/default/files/se-single-phase-HD-wave-inverter-setapp-datasheet.pdf (accessed: June 2022).

[35] F. Baumgartner, *The Performance of Photovoltaic (PV) Systems, Chapter 5: Overall Efficiency Of Grid Connected Photovoltaic Inverters (References To EN 50530:2010+A1:2013)* (Ed: N. Pearsall), Elsevier, London, GB **2017**.

[36] W. Bower, C. M. Whitaker, W. Erdman, M. B. Behnke, M. Fitzgerald, Technical report, Sandia National Laboratories **2004**.

[37] SMA Solar Technology AG, files.sma.de/downloads/SB30-60-DS-en-52.pdf (accessed: June 2022).

[38] SolarEdge Technologies Inc., www.solaredge.com/sites/default/files/se-single-phase-16a-inverter-datasheet.pdf (accessed: June 2022).

[39] International Energy Agency (IEA), iea-pvps.org/research-tasks/performance-operation-and-reliability-of-photovoltaic-systems/ (accessed: June 2022).

[40] International Electrotechnical Commission (IEC), www.iec.ch/dyn/www/f?p=103:14:0:::::FSP_ORG_ID,FSP_LANG_ID:2749,25 (accessed: June 2022).